

Interannual correlations between sea surface temperature and concentration of chlorophyll pigment off Punta Eugenia, Baja California during different remote forcing conditions

H. Herrera-Cervantes^{1,*}, S. E. Lluch-Cota², D. B. Lluch-Cota², and G. Gutiérrez-de-Velasco¹

1. Unidad La Paz, Centro de Investigación Científica y de Educación Superior de Ensenada (CICESE), La Paz, Baja California Sur 23050, México.

2. Centro de Investigaciones Biológicas del Noroeste (CIBNOR). Instituto Politécnico Nacional 195, La Paz, Baja California Sur 23096, México.

*Corresponding author: e-mail: hherrera@cicese.mx

ABSTRACT

5 Interannual correlation between satellite-derived sea surface temperature (SST) and
surface chlorophyll *a* (Chl-*a*) are examined in the coastal upwelling zone off Punta Eugenia
on the west coast of the Baja California Peninsula, an area that has been identified as
having intense biological productivity and oceanographic transition between mid-latitude
and tropical ocean conditions. We used empirical orthogonal functions (EOF) analysis
10 separately and jointly on the two fields from 1997 through 2007, a time period dominated
by different remote forcing; ENSO conditions (weak, moderate and strong) and the largest
intrusion of subarctic water reported in the last 50 years. Coastal Upwelling Index
anomalies (CUI) and the Multivariate ENSO Index (MEI) were used to identify the
influence of local (wind stress) and remote (ENSO) forcing over the interannual variability
15 of both variables. The individual EOF₁ analysis showed the greater variability of SST and
Chl-*a* offshore, their corresponding amplitude time series presented the highest peaks
during the intrusion of subarctic water (2002-2004) and were significantly correlated with the
MEI ($R_{SST} \approx 0.67$, $P < 0.05$). The joint EOF₁ and the SST–Chl-*a* correlations patterns show
the area where both variables covary tightly; a band near the coast where the largest
20 correlations occurred ($R > |0.4|$) and are mainly regulated by ENSO cycles. This was
revealed when we calculated the homogeneous correlations for periods of El Niño - La
Niña and the intrusion of subarctic water. Both, SST and Chl-*a* showed higher coupling and
two distinct physical-biological responses; On average ENSO influence was observed
clearly along the coast mostly in SST, while the subarctic water influence, were observed
25 offshore and Bahía Vizcaíno, mostly in Chl-*a*. We found coastal chlorophyll blooms off
Punta Eugenia during 2002-2003, an enrichment pattern similar to that observed off the
coast of Oregon. These chlorophyll blooms are likely linked to high wind stress anomalies
during spring and summer 2002, mainly at high latitudes. This observation may provide an
explanation of why Punta Eugenia is one of the most important Biological Action Centers
30 on the Pacific coast.

Keywords: Interannual correlations, EOF, physical-biological responses, subarctic water

1. Introduction

Continuous oceanographic observations carried out on the west coast of Baja California by the CalCOFI (California Cooperative Oceanic Fisheries Investigations) and IMECOCAL (Mexican Research of the California Current) programs have helped define the region of Punta Eugenia (Figure 1) as an oceanographic transitional zone (Durazo and Baumgartner, 2002), characterized by the interaction of subarctic and tropical waters (Almazán-Becerril, et al., 2012) as a result of the convergence of the southern part of the California Current (CC) and the North Equatorial Current (NEC). Its shelf is about 50-90 km wide, including Bahía Vizcaíno, this become narrow and almost disappears off Punta Eugenia (González-Rodríguez, et al., 2012). The area is also influenced by warm and dense water originating in the Gulf of California (Parés-Sierra et al., 1997), creating a complex mixing zone between coastal and oceanic flows and intense mesoscale variability characterized by a complex pattern of filaments, meanders, and semi-permanent eddy structures (Gallaudet and Simpson, 1994). These structures carry nutrient-rich coastal waters to deep areas, causing important seasonal variability and inter-annual and long-term changes in the mean field of variables as SST and chl-a (Espinosa-Carreón, et al. 2004).

Seasonal wind forcing over the Punta Eugenia area is controlled regionally by the position and intensity of the North Pacific high pressure and the California semi-permanent low thermal (Parés-Sierra, et al., 1997). This wind pattern generates an intense coastal upwelling process that, together with the local contribution of the coastal lagoons (Guerrero Negro, Ojo de Liebre, and San Ignacio), produces one of the most important Biological Action Centers of the western coast of North America, which is characterized by above average pigment concentrations (Lluch-Belda et al., 2000). The coastal ecosystem of this region is a natural refuge and a feeding and breeding area for many ecological and

commercially important species (gray whale, sea turtles, spiny lobster, abalone, and clams). Maintenance of this ecosystem is based on three factors: rich coastal waters associated with an intense upwelling regime, successful implementation of cooperatives to safeguard existing resources, and relative isolation. These factors help support the fishery and natural resources in this area, which includes red lobster (value of 65 million dollars annually; Vega, et al. 2010; SAGARPA, 2011), abalone (value of 26 million dollars annually; SAGARPA, 2001), and extraction of salt by solar evaporation (7,000 tons annually; SEMARNAT, 1997) contributing to the economy of the entire peninsula.

10 Oceanographic features off the west coast of the Baja California Peninsula are dramatically affected by global-scale ENSO and interdecadal variability. El Niño events have a negative effect on fisheries: an increase in SST, sea level height, change in composition of the zooplankton community, and microbial pollution (Strub and James, 2002, Lavaniegos et al., 2002, Boehm et al., 2004). Larval reproduction and embryonic development of spiny lobster (*Panulirus interruptus*) are heavily impacted by El Niño events because the onset and duration of larval development is accelerated or delayed, which dramatically reduces the captures in this region (Vega, 2003). Carreón-Palau et al. (2003) and Muciño-Días et al. (2004), describe serious decline of abalone because survival, growth, and larval recruitment are heavily dependent on cooler environmental conditions. These relationships between biological and environmental factors demonstrate strong physical-biological coupling in this region.

Climate effects on SST and Chl-a in this coastal environment are well documented here due to more than a decade of satellite measurements (1997-2007). This period has been identified by Behrenfeld, et al., 2006 as the potential transition to permanent El Niño condition in a warmer climate state that include the different ENSO conditions (weak, moderate and strong) beginning with an strong El Niño/La Niña cycles between 1997 and 1999, followed by weak El Niño between 2002- 2004, and finally a

moderate El Niño during 2006-2007. Additionally, during the 2002-2004 the California Current System (CCS), remained in the cold phase, a state it has maintained since the 1999 La Niña phase with the constant permanence of the largest intrusion of subarctic water reported in the last 50 years, which is characterized as a cold and fresh anomaly in the upper halocline (Huyer, 2003, Goericke, et al., 2005).

In this study, we explored the interannual covariance between SST and Chl-*a* off Punta Eugenia, an adequate area as a reproductive habitat due to high levels of biological production and its responses to two different large scale processes; the ENSO cycles and the intrusion of subarctic water. Individual and joint empirical orthogonal functions (EOF) analyses were used to extract the principal modes of interannual variability and correlations patterns to analyze statistically the temporal and spatial coupled modes of variability between SST and Chl-*a* and their response to warming and cooling climate processes. Additionally, we examine time series of coastal anomalies of SST, Chl-*a* and wind stress to observe the propagation of the ENSO signals and subarctic water intrusion during two different time periods; 1997-2007 and 2002-2004.

2. Data and Methods

The data used in this analysis are monthly composites of SST and Chl-*a* satellite images covering from September 1997 through December 2007 for an area from 26–29°N and 113–116°W, centered at Punta Eugenia (see Figure 1). This data are derived from Advanced Very High Resolution Radiometer (AVHRR-Pathfinder) sensor for SST and sea-viewing wide field-of-view sensor (SeaWiFS) for Chl-*a*, available at their respective addresses (<http://podaac.jpl.nasa.gov/> and <http://oceancolor.gsfc.nasa.gov/SeaWiFS>). The initial resolution of 9 × 9 km for Chl-*a* was sampled at a 4 × 4 km cell size to generate monthly averages with the same spatial resolution for SST, rotating and orienting the images along the coast. A large data set containing coincident in situ chlorophyll

measurements has been used to evaluate the accuracy, precision and suitability of ocean color chlorophyll algorithms used by SeaWiFS (O'Really, J. E., et al., 2000). CalCOFI in situ data set covering the CCS region was used for development these algorithms. Kahru and Mitchell (2001) as well as Mitchell (2004) have shown that the CalCOFI and IMECOCAL region are ideal locations to evaluate surface Chl-a concentration from ocean color sensors nevertheless, they found significant discrepancies between satellite-derived Chl-a data and in-situ values at near-shore CalCOFI stations.

Indices of the intensity of large-scale, wind-induced coastal upwelling (CUI) are generated by the NOAA/NMFS Pacific Fisheries Environmental Laboratory (PFEL) at 15 standard locations along the west coast of North America (Schwing et al., 1996; <http://www.pfeg.noaa.gov/>). We used the CUI centered on 27°N, 116°W, as representative of the Punta Eugenia coastal region, filtering out the seasonal cycle by subtracting the corresponding climatological monthly average (CUI interannual anomalies time series). ENSO activity was represented by The Multivariate El Niño Index (MEI), a measure of the variability of the Pacific (Wolter and Timlin, 1993, Behrenfeld et al., 2006). Monthly MEI data were obtained from the Climate Prediction Center of the National Center of Environmental Prediction at the National Oceanic and Atmospheric Administration (NOAA-CPC-NCEP; <http://www.cpc.ncep.noaa.gov/>). Finally, the CUI and MEI indices were normalized by dividing the time series by its standard deviation and smoothed using a running mean of three months to reduce small scale and short term variability.

The monthly composite images of SST and Chl-a, were arranged in matrices $M(x, t)$ for each variable, where x stands for the cells of each image and t stands for each month between September 1997 and December 2007 (NT images). To remove the annual and semiannual signals by subtracting a fitted (least squares) periodic function from each pixel time series, the periodic function was defined as:

$$F(t) = A_0 + A_1 \cos(w_1 t - \varphi_1) + A_2 \cos(w_2 t - \varphi_2), \quad (1)$$

where A_0 is the annual mean, A_1 , w_1 , and φ_1 are the amplitude, frequency, and phase of the annual signal and A_2 , w_2 , and φ_2 are the equivalent of the semi-annual signal. Next, we obtained the matrices of SST and Chl-*a* anomalies (interannual variability), subtracting
5 from each time series of each cell, its corresponding fitted periodic function (Eq. 1) as:

$$\mathbf{A}(x, t) = \mathbf{M}(x, t) - \mathbf{F}(x, t) \quad (2)$$

Each matrix was transformed into normalized anomalies $NA(x, t)$ by dividing $A(x, t)$ series by its standard deviation (series were re-scaled to make them comparable). The resulting $NA(x, t)$ matrices of both variables were used in the individual EOF analysis to
10 identify the dominant modes of SST and Chl-*a* interannual variability and its evolution over time (principal components). Joint EOF are calculated from the covariance matrix constructed from both variables (SST and Chl-*a*) to highlight how they covary with each other, forcing them to have the same temporal variability but different patterns of spatial variability (Wilson and Adamec, 2001).

15 To isolate and spatially localize important coupled modes of variability, correlations between SST and Chl-*a* are examined for the time period September 1997 to December 2007. Homogeneous correlations (Bretherton, et al., 1992) are calculated for two subsets of the time series; between September 1997 to December 1999 to the ENSO coupled signal and between January 2002 to December 2003 to the subarctic water
20 intrusion signature. High homogeneous correlations indicate the regions that contribute the most to the temporal variability. The statistical significance and the critical value (R_{crit}) in these correlations were calculated using the effective number of degrees of freedom rather than the number of months of data available (see e.g., Davis, 1976, Chelton, 1982 and Tremberth, 1983).

25 MEI and CUI series were obtained from the NOAA Climate Prediction Center (CPC-NCEP-NOAA) website (<http://www.cpc.ncep.noaa.gov>) and from the Pacific Fisheries Environmental Group (PFEG) website (<http://www.pfeg.noaa.gov/>). We note that,

though these indices summarize variability over different regions and the correlation between them are not large, wind data used to build monthly CUI anomalies in this region are strongly affected by ENSO events and are not completely independent (Storch and
5 Zwiers, 1999). Finally, to observe the presence of the different ENSO signals within the ~30 km closest to the coast of the study area, we built time plots (Hovmöller diagrams) based on time series of coastal SST and Chl-*a* anomalies data between September 1997 and December 2007. Additionally, the presence of the intrusion of subarctic water closest to the coast of North America (22°N-45°N) and its relationship with the Chl-*a* and wind
10 forcing, were analyzed based on Hovmöller diagrams of Chl-*a* and wind stress anomalies between January 2002 and December 2003. For this last analysis we used Chl-*a* weekly 18 x 18 km pixel arrays composites filtering out the seasonal cycle subtracting the Chl-*a* weekly climatology provided by the SeaWiFS Project of NASA Goddard Space Flight Center website at <http://oceancolor.gsfc.nasa.gov/>. The wind stress anomalies (N m^{-2}) was
15 calculated in the same way that the matrices of SST and Chl-*a* used in the individual EOF analysis, using monthly mean ocean surface wind in a $0.25^\circ \times 0.25^\circ$ pixel array composited provided by the Cross-Calibrated Multi-Platform (CCMP) project website at <http://podaac.jpl.nasa.gov/dataset/> and re-binned into 18x18km to have the same spatial resolution used in Chl-*a*.

20

3. Results

To determine the regions off Punta Eugenia where SST and Chl-*a* have the largest seasonal fluctuations, the standard deviation (STD) variability is calculated for each monthly time series of the satellite-derived SST(x, \bar{t}) and Chl-*a* (x, \bar{t}) observations (Figure
25 2). Both patterns had large gradients along the coast and the largest seasonal fluctuations in SST ($>3^\circ\text{C}$) and Chl-*a* ($>1\text{mg m}^{-3}$) near to the coast, mainly south of Punta Eugenia. The deep zone, presented the lowest values, this included Bahía Vizcaíno where the barotropic

circulation associated to a semi-permanent anticyclonic gyre (Palacios-Hernandez, et al., 1996) could mask the amount of biological productivity. This pattern is consistent with near shore eutrophic conditions and/or oligotrophic conditions farther offshore (Kahru and Mitchell, 2000). The bottom panels represent the seasonal cycle and show the time plot of SST, Chl-a, and CUI [space-average $SST(x, \tilde{t})$ and $Chl-a(x, \tilde{t})$ and CUI monthly time series], all dominated by strong annual peaks, although large interannual changes were still evident. High peaks of Chl-a and CUI (spring –summer) seem to show a trend of increasing annual maxima, mostly during 2002-2003, Kahru and Mitchel (2012), using monthly composites of four ocean color sensors-derived Chl-a dataset, showed a similar behavior in coastal areas off Baja California. The annual cycle for each of the three parameters reveals significant coincidences between them.

The interannual variability of SST and Chl-a off Punta Eugenia is defined by a single dominant mode in both EOF analysis, these being statistically different as their error bars (not showed) do not overlap with theirs neighboring (North et al., 1982). Figure 3 shows the spatial patterns and principal components for mode 1 of the individual EOF analyses (surface plot of the EOF_1 loadings), which account for 78% and 45% of the total variance for SST and Chl-a (with the sign-reversed) respectively. Both spatial patterns showed strong gradients along the coast and high loadings were observed offshore (deep region). The pattern of high SST variability (3a), coincide with the pattern of high Chl-a variability (3b), whereas low SST and Chl-a variability occurred near the coast. The principal components showed a major correlation with the MEI. The correlations between the principal components of individual EOF analyses (SST and Chl-a) and the normalized time series of MEI and CUI anomalies are presented in Table 1. The correlation between the principal components of SST and MEI were high ($R = 0.67$, $P < 0.05$) and low for Chl-a ($R = -0.13$), while the correlation between the principal components of SST and Chl-a and CUI was low ($R = -0.13$ and $R = 0.20$ respectively), suggesting that the interannual

correlation of both variables is strongly dominated by SST and forced principally by different ENSO conditions (weak, moderate, and strong), except during 2002-2004 when the principal component of Chl-*a* (SST) showed highest positives (negative) amplitudes.

5

Figure 4 shows the spatial pattern of the first mode of the joint EOF₁ analysis for SST and Chl-*a* (4a, 4b), accounting for 80% of the total variance. The amplitude time series corresponding to the joint EOF₁ is not shown since it is virtually identical to those of individual SST components showed in figure 3c, having correlation of 0.98 (see Table 1).

10 The Joint spatial modes (SST and Chl-*a*), differ to those of the individual EOF₁ (3a, 3b). The primary difference is that the coastal and northern region dominates more in the joint EOF, mostly in the chlorophyll mode (4b) where Bahía Vizcaíno shows the largest spatial loadings. In the joint mode low variability corresponds to the depth and southern region as a continuous feature. The spatial distribution of the correlation coefficient between monthly
15 anomalies of SST and Chl-*a* (4c), present the area where both parameters strongly co-vary. This area (a band parallel to the coast) is enclosed with the highest correlations ($|R| > 0.25$) and joint EOF₁ scores (>2.0) of the SST (4a). Correlations above $R_{crit} (P<0.05) = 0.211$, i.e., the strongest negative correlation in the blue areas is statistically significant ($P<0.05$). Correlations that are not statistically significant at the 95% level are shaded light
20 blue.

Figure 5 shows contours of mean homogeneous correlation calculated for three subset of the time series in both SST and Chl-*a* respectively overlaid on (a) the spatial correlation pattern (Figure 4c) and (b) the chlorophyll mode of the individual EOF₁ analysis (Figure 3b) to assess what regions dominate during the El Niño period (September 1997 to
25 December 1998), La Niña period (September 1998 to December 2000) and the intrusion of subarctic water period (January 2002 to December 2003). For both SST and Chl-*a*, a narrow area confined along the coast dominates during El Niño and La Niña: (solid and

dotted contours in Figure 5a). The combination of the mean sets of homogeneous correlation distributions is virtually identical to the spatial correlation and the joint SST mode patterns, meaning that the physical-biological coupling showed in the coastal region, is driven by both increase and decrease of SST and chlorophyll during ENSO cycles.

In contrast, the region that dominate significantly during the intrusion of subarctic water period for both SST and Chl-a was found to occur with a mean homogeneous correlation of >0.6 (solid contours in Figure 5b) and are located all in the deep zone and in Bahía Vizcaíno, they occur in the same region where individual EOF patterns show the high variability mainly in the chlorophyll mode (Figure 3b). These results indicate that the individual variability pattern of both parameters were driven more by the intrusion of subarctic water than by ENSO cycles, and contributed little to the coupled mode. The sets of homogeneous correlation in Figure 5 delineate the regions that contribute the most to the individual and coupled modes during different remote forcing; the deep region and coastal area respectively.

Figure 6 shows the time series of (a) the MEI index and CUI anomalies, both compared with the temporal evolution of (b) SST and (c) Chl-a coastal anomalies plotted in two Hovmöller diagrams (*i.e.*, time series of coastal pixels plotted as contours) from 26°N (at the bottom of the diagrams) to the north of Bahía Vizcaíno (at the top, the black line at the middle indicates the position of Punta Eugenia on the coast). Monthly CUI anomalies time series are partially impacted by the different ENSO cycles (weak, moderate and strong), in phase but negatively correlated with the MEI in most of the time period. Warm (cold) ENSO events are indicated by orange (blue) bars and are associated with positive (negative) SST coastal anomalies. Panels b and c show that positive and negative anomalies of SST and Chl-a respectively are associated with ENSO events. Strong anomalies in the southern of Punta Eugenia are transmitted to the Bahía Vizcaino with a slight attenuation (1999-La Niña, 2007-El Niño), except during the 2002-2004 period when

a cold event strongly affected Bahía Vizcaíno, masking the presence of the weak El Niño event. The maximum SST anomalies ($\sim 3^\circ\text{C}$) and Chl- *a* ($\sim -2\text{ mg m}^{-3}$) occurred during the strong 1997-1998 El Niño event, thereby causing a sign reversal during the 1999-2000 La Niña conditions occurred mainly in southern part of Punta Eugenia ($\sim -2^\circ\text{C}$ and $\sim 1.8\text{ mg m}^{-3}$, respectively). During the weak 2002-2004 El Niño event, both parameters showed unusual behavior along the coast; negative SST anomalies (-2.5°C) and positive Chl- *a* (2 mg m^{-3}) mainly north of Punta Eugenia. Finally, during the moderate 2006-2007 El Niño, the SST surface anomalies showed the typical influence of a warm ENSO event along the coast, while the Chl-*a*, continued to have positive anomalies.

Figure 7 shows the relationship between the wind stress and Chl-*a* anomalies during the intrusion of subarctic water period (January 2002 to December 2003) in an area closest to the coast of North America (22°N - 45°N). Latitude-time plots of (a) anomalies of monthly wind stress (magnitude and direction; $\text{N m}^{-2} \times 10^{-2}$) showed a weak wind stress anomalies in early 2002, increasing in intensity during spring-summer of 2002 (onshore direction). Anomalous wind stress along the Northeast Pacific coast may drive enhanced coastal upwelling and anomalous Ekman transport along the immediate coast (Taylor, et al., 2008). Coastal Chl-*a* anomalies (b) showed in detail that the southern coast, which includes since the study area (shaded in green) to the tip of the peninsula, presented high positives anomalies in Chl-*a* ($>2.5\text{ mg m}^{-3}$). It should be noted that Chl-*a* signal off Punta Eugenia, reach bloom conditions compared to that found north of 42°N (off Oregon coast), where the presence of the cold and fresh subarctic water masses in the CCS was first noticed (Kosro, 2003, Freeland et al., 2003, Goericke et al., 2005). High positive Chl-*a* coastal anomalies, continued off Baja California during spring and summer, 2003 without any significant delay or attenuation by the co-occurring 2002-2003 El Niño event (Bograd and Lynn, 2003, Durazo, et al., 2005), while wind stress anomalies showed a pronounced decline.

4. Discussion

In this study, we used EOF analysis both separately and jointly over satellite-driven SST and Chl-*a* anomaly data off Punta Eugenia, region with high levels of biological productivity that is associated with wind-driven upwelling process (González-Rodríguez, et al., 2012, Lluch-Belda, 1999) which has allowed us a wide-ranging view of the biophysical coupling during several ENSO events and the largest intrusion of subarctic water reported during 2002-2003. Moreover, by relating each SST and Chl-*a* series within ~30km closest to the coast off Punta Eugenia to two independent variables, MEI and CUI and we followed the coastal signal of the Chl-*a* related to the intrusion of subarctic water since 45°N to 22°N. To our knowledge, this is the first time that physical-biological covariability driven by remote forcing (tropical and subarctic origin) off Punta Eugenia has been examined at this level of detail.

The spatial patterns of individual EOF₁ (Figures 3a and 3b) showed that the interannual variability of SST and Chl-*a* are not homogeneous and have a strong gradient along the coast. Although both patterns are similar, its principal components are markedly different ($R \approx 0.21$; see Table 1). The principal components of the SST mode compared with the MEI showed that they are statistically significant ($R = 0.67$, $P < 0.05$), except with the CUI anomalies time series ($P > 0.05$, see Table 1). This may indicate that were forced at the beginning of the time period by ENSO-related events but during the 2002–2004 by the large intrusion of subarctic water reported in the last 50 years (Venrick et al., 2003, Bograd and Lynn, 2003, and Durazo et al., 2005, Goericke, et al, 2005) which masked the presence of the El Niño event of this period. Chl-*a* reached the highest peak of variability during this period (Figure 3c), suggesting that Chl-*a*, unlike SST, was mostly affected by the intrusion of subarctic water, in this case the individual variability patterns of both variables are defined as the subarctic water mode. The four time series showed similar behavior during 1999–2006, a period defined by sustained warming and increasing MEI

values (Berenhfeld et al., 2006) resulting in an increase (decrease) in SST (Chl-*a*) and vice versa. These observations are consistent with the overall decreasing trend of Chl-*a* off Southern Baja California, possibly associated to a weaker of El Niño events (Kahru, et al.,
5 2012).

In contrast, the spatial patterns of joint EOF₁ showed that the SST–Chl-*a* interannual covariation off Punta Eugenia is the ENSO mode. The spatial pattern of SST (Figure 4a) showed an intense variability within the nearshore band, while the spatial pattern for Chl-*a* (4b), differ little by having high loadings more evenly centered northern of
10 Punta Eugenia, including Bahía Vizcaíno. The spatial pattern of joint SST mode is identical to the correlation map between SST and Chl-*a* (Figure 4c), having spatial correlation of $R = |0.98|$). During El Niño events, coastal trapped waves (Durazo and Baumgartner, 2002, Dever and Winant, 2002, Jacobs et al., 1994) reach the Baja California Peninsula coast accompanied by meandering poleward flow, positive SST
15 anomalies increases the sea surface height that deepen the nutricline and reduce the availability of nutrients to the euphotic zone. While the signals associated with La Niña events are accompanied by positive anomalies of Chl-*a* associated with an intensification of the north winds, from which the upwelling events raise the nutricline and thus increase the availability of nutrients in the coastal region of Baja California (Espinosa-Carreón, et
20 al., 2012, Chavez, et al., 1999, Wooster and Hollowed, 1995). The correlation pattern, suggests that the different physical-biological responses to events as the ENSO oscillations arise from a combination of ecological and physical dynamics (Wilson and Adamec, 2001), suggesting a high biophysical coupling off Punta Eugenia during ENSO cycles (Espinosa, et al., 2004).

25 In a similar fashion, we overlaid the mean homogeneous correlation calculated for the periods El Niño, La Niña and the intrusion of subarctic water on the spatial correlation pattern and the chlorophyll mode of the individual EOF₁ analysis (Figure 6). There are no

significant changes between the mean homogeneous correlation distribution during the El Niño and La Niña time period (solid and dotted contours). The region dominated for both events is a narrow coastal band that coincide with those of the spatial distribution of intense co-variability and the high correlations between SST and Chl-*a* (Figure 5c), which reflects the stronger representation of the coastal zone in the ENSO mode. The high correlations along the coast coincident with the region where intense coastal wind-driven upwelling and complex mesoscale variability are found (Espinosa-Carreón, et al., 2012, Gonzalez-Rodríguez, et al., 2012) and where the propagation of coastal waves has been observed during the El Niño event (Parés-Sierra and O'Brien, 1989, Durazo and Baumgartner, 2002). The homogeneous correlation distribution calculated during the intrusion of subarctic water delimited a different area (solid contours in Figure 5b). The mean homogeneous correlation for both variables dominate a broad area centered in the western basin where the depth is > 1000 m (Figure 1) and over Bahía Vizcaíno where higher homogeneous correlation delineate the region associated with strengthening of Chl-*a* during the intrusion of subarctic water. These regions contributes significantly to the spatial patterns of individual EOF₁ when analyzed over the entire time series (Figure 3a,b).

The SST and Chl-*a* anomaly evolutive diagrams (Figure 5b, c) showed that, MEI and CUI anomalies are not related with the intrusion of subarctic water. Espinosa-Carreón *et al.* (2004) suggested that on an interannual timescale, changes in the monthly CUI anomalies do not appear to be the primary source of variability in the oceanic parameters like that SST and Chl-*a*, since removing the seasonal component results in low correlation values (see Table 1). The chlorophyll bloom of 2002–2003 seemed greater than during the strong 1999–2000 La Niña, evidencing that the distribution of biological groups in areas as far south as 28°N were influenced mostly by the intrusion of water of northern origin, than by events of both local and equatorial origin (upwelling and ENSO event). These conditions, driven by southern part of the California Current (Bograd and Lynn, 2003;

Durazo et al., 2005), caused a reversal in environmental conditions opposite to the ocean Pacific variability shown by the MEI in this period. Durazo et al., 2005 observed in surface, the presence of zooplankton groups (salps) associated with an intrusion of subarctic water but also at depths of 100 m zooplankton groups (chaetognaths) was associated with water of tropical origin that accompanies El Niño events,.

The evolution of exceptionally high Chl-a concentration along the western coast of North America during the intrusion of subarctic water period (2002-2003), can be observed in Figure 7. This was extended toward the equator more than 3000 km (from 45°N to 22°N), coastal area where the extension of the continental shelf, the geometry of the coastline and the local processes (wind-driven coastal upwelling and advection) play an important role in modulating the productivity. Wind stress anomalies developed north of 35°N and strengthened during spring and summer 2002, coinciding with positives Chl-a anomalies observed along the North America coast. This could be associated with onshore large scale advection induced by winds in the central Pacific (Chelton and Davis, 1982) or anomalous Ekman transport that may drive enhanced coastal upwelling and/or more vigorous along-coast currents (Taylor, et al., 2008). It is noteworthy that positives Chl-a anomalies observed off Punta Eugenia during spring and summer 2002, could be compared to those observed north of 42°N, both could be result of the strong west wind stress anomalies and enhanced coastal upwelling developed in spring-summer 2002, increasing levels of pigment concentration above the average for the coastal zone. This bloom of positives Chl-a anomalies occurs again during summer 2003 and is coincident with the peaks of amplitude time series of the Chl-a individual EOF₁ scores (Figure 3c).

Our study supports the notion that changes in Chl-a concentration could be due to other factors such as decadal variability, changes in grazing pressures on the phytoplankton (Lavaniegos et al., 2006, Wilson and Adamec, 2001) that may cause impact on biological communities located along the coast. Gaxiola et al. (2008), using data

obtained during IMECOCAL cruises (2001-2007), observed that, the intrusion of subarctic water represented by an anomalous low salinity condition in the southern sector of the California current appears to be coupled with the 2002-2006 warm phase of the Pacific Decadal Oscillation Index (PDO). Neither the local upwelling (represented by the CUI anomalies) nor the zonal Ekman drift velocity used as a proxy for coastal upwelling, showed signals associated with the presence of the intrusion of subarctic water. In this case, the positives signals of wind stress developed along the coast, were agreement with the bloom of the Chl-*a*, mainly northern of 35°N (Figure 7).

10

6. Conclusions

Unlike the data gathered during oceanographic cruises, the temporal and spatial resolution of satellite-derived SST and Chl-*a* data allowed for observation (both separately and jointly on the two fields) of the physical-biological coupling of very near shore environments during large scale processes that affected the region off Punta Eugenia. This region of intense biological productivity and oceanographic transition is highly influenced by the intrusion of subarctic water and by subtropical signatures triggered by poleward flow (e.g. ENSO cycles). The spatial patterns of individual EOF₁ were forced mainly by an unusual enhanced onshore transport of subarctic water during the period 2002-2004, defined by Goericke, et al., 2005 as a cold phase of the CCS, a state it has had since the 1999 La Niña phase. While the physical-biological coupling was forcing mainly by interannual variability of equatorial origin (ENSO events) tightly observed in an alongshore band of ~40 km wide. Higher homogeneous correlation calculated during El Niño and La Niña time period delineated the regions that contribute the most to the ENSO mode.

25

Although, ENSO events have dominated the area for a long time, the presence of the intrusion of subarctic water off Punta Eugenia, has dominate the individual interannual

variability of both SST and Chl-a variables. This remote forcing results in a large-scale chlorophyll bloom that extends for more than 3000 km of the Northeast Pacific coast (22°N-45°N) showing that Punta Eugenia is one of the most important Biological Action Centers (BAC) of the western coast of North America with levels of pigment concentration comparable to that found at higher latitudes (Oregon coast). These results successfully support the data from previous hydrographic surveys (CaLCOFI and IMECOCAL programs) off Baja California.

10 **Acknowledgments.** Ira Fogel and M.V. Cordoba-Matson of CIBNOR provided editorial improvements. We thank the Pathfinder and SeaWiFS Projects and the NASA Physical Oceanography Distributed Active Archive Center for the production and distribution of AVHRR-SST and SeaWiFS data. This research was funded by SAGARPA-CONACYT grants 2009-113C. Additional thanks go to the anonymous reviewers who gave
15 valuable comments on an earlier draft of manuscript.

REFERENCES

- Almazán-Becerril, A., Rivas, D. García-Mendoza, E.: The influence of mesoscale physical structures in the phytoplankton taxonomic composition of the subsurface chlorophyll maximum off Baja California, *Deep-Sea Research I*, 70, 91-102, 2012
- 20 Behrenfeld M. J., O'Malley, R. T., Siegel, D. A., McClain, C. R., Sarmiento, J. L., Feldman, G. C., Milligan, A. J., Falkowski, P.G., Letelier, R.M., Boss E. S.: Climatic-driven trends in contemporary ocean productivity, *Nature*, 444, 752-755, 2006.
- 25 Bretherton, C. S., Smith, C., Wallace, J. M.: An intercomparison of methods for finding coupled patterns in climate data. *Journal of Climate*, 5, 541-560, 1992.

- Boehm, A. B., Lluch-Cota, D. B., Davis, K. A., Winnan C. D., Monismith, S. G.: Covariation of coastal water temperature and microbial pollution at interannual to tidal periods, *Geophys. Res. Lett.*, 31, L06309, doi:10.1029/2003GL019122, 2004.
- 5 Bograd, S. J., Lynn, R. J.: Anomalous subarctic influence in the southern California Current during 2002, *Geophys. Res. Lett.*, 30, 8020, doi: 10.1029/2003GLO17446, 2003.
- Carreón-Palau, L., Guzman Del P. S. A., Belmar, J. P., Carrillo, J. L. Herrera, R. F.:
Microhábitat y biota asociada a juveniles de abulón *Haliotis fulgens* y *Haliotis*
10 *corrugata* en bahía Tortugas, Baja California Sur, México, *Ciencias Marinas*, 29, 325-341, 2003.
- Chavez, F. P., Strutton, P. G., Friederich, G. E., Feely, R. A., Feldman, G. C., Foley, D. G., McPhaden, M. J.: Biological and chemical response of the equatorial Pacific to the 1997-1998 El Niño, *Science*, 286, 2126-2131, 1999.
- 15 Chelton, D. B., Davis, R. E.: Monthly mean sea level variability along the west coast of North America, *J. Phys. Oceanogr.*, 12, 757-784, 1982.
- Chelton, D. B.: Statistical reliability and the seasonal cycle: comments on "Bottom pressure measurements across the Antarctic Circumpolar Current and their relation to the wind", *Deep-Sea Research*, 29, IIA, 1381-1388, 1982.
- 20 Davis, R. E.: Predictability of sea surface temperature and sea level pressure anomalies over the North Pacific Ocean, *J. Phys. Oceanogr.*, 6, 249-266, 1976.
- Dever, E. P. and Winant, C. D.: The evolution and depth structure of shelf and slope temperatures and velocities during the 1997–1998 El Niño near Point Conception, California, *Prog. Oceanogr.*, 54, 77–103, 2002.
- 25 Durazo, R. and Baumgartner, T. R.: Evolution of oceanographic condition off Baja California: 1997-1998, *Prog. Oceanogr.* 54, 7-31, 2002.

- Durazo, R., Gaxiola-Castro, G., Lavaniegos, B., Castro-Valdez, R., Gómez-Valdez, J. and Mascarenhas Jr, A.S.: Oceanographic conditions off the western Baja California coast, 2002–2003: A weak El Niño and subarctic water enhancement, *Ciencias Marinas*. 31, 537–552, 2005.
- 5
- Espinosa-Carreón, L., Strub, P. T., Beier, E., Ocampo-Torres, F. and Gaxiola-Castro, G.: Seasonal and interannual variability of satellite-derived chlorophyll pigment surface height, and temperature off Baja California, *J. Geophys. Res.*, 109, C03039, doi: 10.1029/2003JC002105, 2004.
- 10
- Espinosa-Carreón, L., Gaxiola-Castro, G., Beier, E., Strub, P. T. and Kurczyn, J. A.: Effect of mesoscale processes on phytoplankton chlorophyll off Baja California, *J. Geophys. Res.*, 117, C04005, doi: 10.1029/2011JC007604, 2012.
- Freeland, H. J., Gatién, G., Huyer, A. and Smith, R.L.: A cold halocline in the northern California current: an invasion of subarctic water, *Geophys. Res. Lett.* Doi: 10.1029/2002GL016663, 2003.
- 15
- Gallaudet, T. C. and Simpson, J. J.: An empirical orthogonal function analysis of remotely sensed sea surfaced temperature variability and its relations to interior oceanic processes off Baja California. *Remote Sens. Environ*, 47, 374–389, 1994.
- Gaxiola-Castro, G.; Durazo, R., Lavaniegos, B., De-la-Cruz-Orozco, M.E., Millán-Nuñez, E., Soto-Mardones, L. and Cepeda-Morales, J.: Pelagic ecosystem response to interannual variability off Baja California, *Ciencias Marinas*. 34 (2), 263-270, 2008.
- 20
- Goericke, R., Venrick, E., Mantyla, A., Bograd, S. J., Schwing, F. B., Huyer, A., Smith, R. L., Wheeler, P. A., Hoff, R., Peterson, W.T., Chavez, F., Collins, C., Marinovic, B., Lo, N., Gaxiola-Castro, G., Durazo, R., Hyrenbach, K. D. and Sydeman, W. J.: The state of the California Current, 2004–2005: Still cool?, *CalCOFI Rep.* 46, 32–71, 2005.
- 25

- González-Rodríguez, E., Trasviña-Castro, A., Gaxiola-Castro, G., Zamudio, L., and Cervantes-Duarte, R.: Net primary productivity, upwelling and coastal currents in the Gulf of Ulloa, Baja California, México: *Ocean Science*. 8, 703-711, 2012.
- 5 Hereu, C. M., Jiménez-Pérez, L. C. and Lavaniegos, B. E.: Effects of the El Niño 1997–1998 and the rapid transition to cool conditions in the winter 1998–1999 on the copepods and salps of the California Current. 3rd International Zooplankton Production Symp., 20–23 May 2003, Gijón Spain, Program and Abstracts, p. 53, 2003.
- 10 Huyer, A.: Preface to special section on enhanced subarctic influence in the California Current, 2002. *Geophys. Res. Lett.*, 30, 15, 8019, doi: 10.1029/2003GL017724, 2003.
- Jacobs, G. A., Hulburt, H. E., Kindle, J. C., Metzger, E. J., Mitchell, J. L., Teague, W. J. and Wallcraft, A. J.: Decade-scale trans-Pacific propagation and warming effect of an El Niño anomaly, *Nature*, 370, 360–363, 1994.
- 15 Kahru, M. and Mitchell, B. G.: Influence of the 1997-98 El Niño on the surface chlorophyll in the California Current, *Geophys. Res. Lett.*, 27, 2937-2940, 2000.
- Kahru, and Mitchell, B. G.: Seasonal and nonseasonal variability of satellite-derived chlorophyll and colored dissolved organic matter concentration in the California Current, *J. Geophys. Res.* 106, NO. C2, 2517-2529, 2001.
- 20 Kahru, M., Kudela, R.M., Manzano-Sarabia, M. and Mitchell, B. G.: Trends in the surface Chlorophyll of the California Current: Merging data from multiple ocean color satellites, *Deep-Sea Research II*, 77-80, 89-98, 2012.
- Kosro, P. M.: Enhanced southward flow over the Oregon shelf in 2002: A conduit for subarctic water, *Geophys. Res. Lett.*, 30, (15), 8023, doi:10.1029/2003GL017436, 25 2003.

- Lavaniegos, B. E., Jiménez-Pérez, L.C. and Gaxiola-Castro, G.: Plankton response to El Niño 1997–1998 and La Niña 1999 in the southern region of the California Current, *Prog. Oceanogr.*, 54, 33–58, 2002.
- 5 Lavaniegos, B. E. and Jiménez-Pérez, L. C.: Biogeographic inferences of shifting copepod distribution during 1997-1999 El Niño and La Niña in the California Current. *Contributions to the Study of East Pacific Crustaceans*, 4, 113–158, 2006.
- Lluch-Belda, D, Elorduy-Garay, J., Lluch-Cota, S. E. and Ponce-Díaz, G.: BAC Centros de Actividad Biológica del Pacífico Mexicano. Centro de Investigaciones Biológicas del
- 10 Noroeste. Centro Interdisciplinario de Ciencias Marinas, Consejo Nacional de Ciencia y Tecnología, La Paz, B.C.S., Mexico, 2000.
- Mitchell. B. G.: Bio-optical measurements and modeling of the California Current and Southern Oceans. Final Report. Scripps Institution of Oceanography, University of California San Diego, La Jolla, CA 92093-0218, 27pp, 2004.
- 15 Muciño-Días, M., Sierra-Rodríguez, O. P., Castro, J. J., Talavera, J. J., Turrubiates, J. R., Caballero, F. and Rivera, J. L.: Estado de las poblaciones de Abulon azul *Haliotis fulgens* y amarillo *H. corrugata* por zona reglamentada en la costa occidental de la península de Baja California. Temporada 2003/2004. Dictamen Técnico. Instituto Nacional de la Pesca. Dirección general de Investigación pesquera en el
- 20 Pacífico Norte. 12pp, 2004.
- North, G. R., Bell, T. L., Calahan, R. F. and Moeng, F. J.: Sampling errors in the estimation of empirical orthogonal functions, *Mon. Weath. Rev.*, 110, 699–706, 1982.
- O'Really, J. E., 24 Coauthors: SeaWiFS Postlaunch Calibration and Validation Analyses, Part 3. Hooker, S. B., Firestone, E. R. (Eds.), NASA Tech. Memo. 2000-206892.
- 25 NASA Goddard Space Flight Center, vol. 11, 49pp., 2000.

- Parés-Sierra, A., Lopez, M. and Pavía, E.: Oceanografía Física del Océano Pacífico Nororiental, in Contribuciones a la Oceanografía Física en México. Monograf. Ser. Vol. 3, Unión Geofísica Mexicana, Puerto Vallarta, México pp. 1-24., 1997.
- 5 SAGARPA: Anuario estadístico de pesca, 2001. Comisión Nacional de Pesca y Acuacultura, México, 2001.
- SAGARPA: Anuario estadístico de pesca, 2011. Comisión Nacional de pesca y Acuacultura, México, 2011.
- SEMARNAT. Secretaria de Medio Ambiente Recursos Naturales: Salitrales de San Ignacio, sal y ballenas en Baja California, México, 1997.
- 10 Schwing, F. B. and Mendelsohn, R.: Increased coastal upwelling in the California Current System, J. Geophys. Res., 102(C2), 3421–3438, doi:10.1029/96JC03591, 1996.
- Soto-Mardones, L., Parés-Sierra, A., García, J., Durazo, R. and Hormazabal, S.: Analysis of the mesoscale structure in the IMECOCAL region (off Baja California) from hydrographic, ADCP and altimetry data, Deep-Sea Research II, 51,785–798, 2004.
- 15 Storch, H. V. and Zwiers, F. W. (Eds.): Statistical analysis in climate research. Cambridge University Press, Cambridge, 1999.
- Strub, P. T. and James, C.: Altimeter-derived surface circulation in the large-scale Pacific gyres. Part 2: 1997–1998 El Niño anomalies, Prog. Oceanogr., 53, 185–214, 2002.
- 20 Taylor, S. V., Cayan, D. R., Graham, N. E., Georgakakos, K, P.: Northerly surface winds over the eastern North Pacific ocean spring and summer, J. Geophys. Res., 113 D02110, doi: 10.1029/2006JD008053, 2008.
- Trenberth, K. E.: Signal Versus Noise in the Southern Oscillation, Monthly Weather Review, 112, 326-332, 1983.
- 25 Vega, A. V.: Reproductive strategies of the spiny lobster *Panulirus interruptus* related to the marine environmental variability off central Baja California, México: management implications, Fisheries Research, 65, 123–135, 2003.

- Vega, A. Treviño, E., Gracia, G., Espinoza-Castro, L. and Zuñiga-Pacheco, C.:
Evaluación de la langosta roja (*Panulirus Interruptus*) en la región centro occidental
de la península de Baja California, mediante modelos dinámicos de biomasa: puntos
5 de referencia y recomendaciones de manejo. Informe de Investigación. Instituto
nacional de la Pesca. 21pp., 2010.
- Venrick, E., Bograd, S., Checkley, D., Cummings, S., Durazo, R., Gaxiola-Castro, G.,
Hunter, J., Huyer, A., Hyrenbach, K., Lavaniegos, B., Mantyla, E. A., Schwing, F.
B., Smith, R. L., Syderman, W. J. and Wheeler, P. A.: The state of the California
10 Current, 2002–2003: Tropical and subarctic influences vie for dominance, CalCOFI
Report, 44, 28–60, 2003.
- Wilson, C. and Adamec, D.: Correlation between chlorophyll and sea surface height in the
tropical Pacific during 1997-1999 El Niño Southern Oscillation event, *J. Geophys.*
Res., 106 (C12), 31,175–31,188, 2001.
- 15 Wolter, K. and Timlin, M. S.: Monitoring ENSO in COADS with a seasonally adjusted
principal component index. Proc. 17th Climate Dynamics Workshop; Norman, OK,
NOAA/NMC/ CAC, NSSL, Oklahoma Clim. Survey, CIMMS and School of
Meteorology. Univ. Oklahoma, Norman, OK pp. 52–57, 1993.
- 20 Wooster, W.S. and Hollowed, A.B.: Decadal scale variations in the eastern subarctic
Pacific. I. Winter ocean conditions. *Climate change and northern fish populations*, R.
J. Beamish (Ed), Canadian Spec. Publ. Fish. Aquatic Sci., 121, 81–85, 1995.

Table 1. Correlations between principal components from different SST and Chlorophyll-a
 EOF1 analysis (Individual and Joint) and MEI and monthly CUI anomalies.

	EOF ₁	EOF ₁	EOF ₁	MEI	CUI
	Ind SST	Ind Chl	Joint		
EOF ₁ Ind SST	1.0				
EOF ₁ Ind Chl	0.21	1.0			
EOF ₁ Joint	0.98	0.97	1.0		
MEI	0.67	- 0.13	0.63	1.0	
CUI	- 0.13	0.20	0.17	- 0.13	1.0

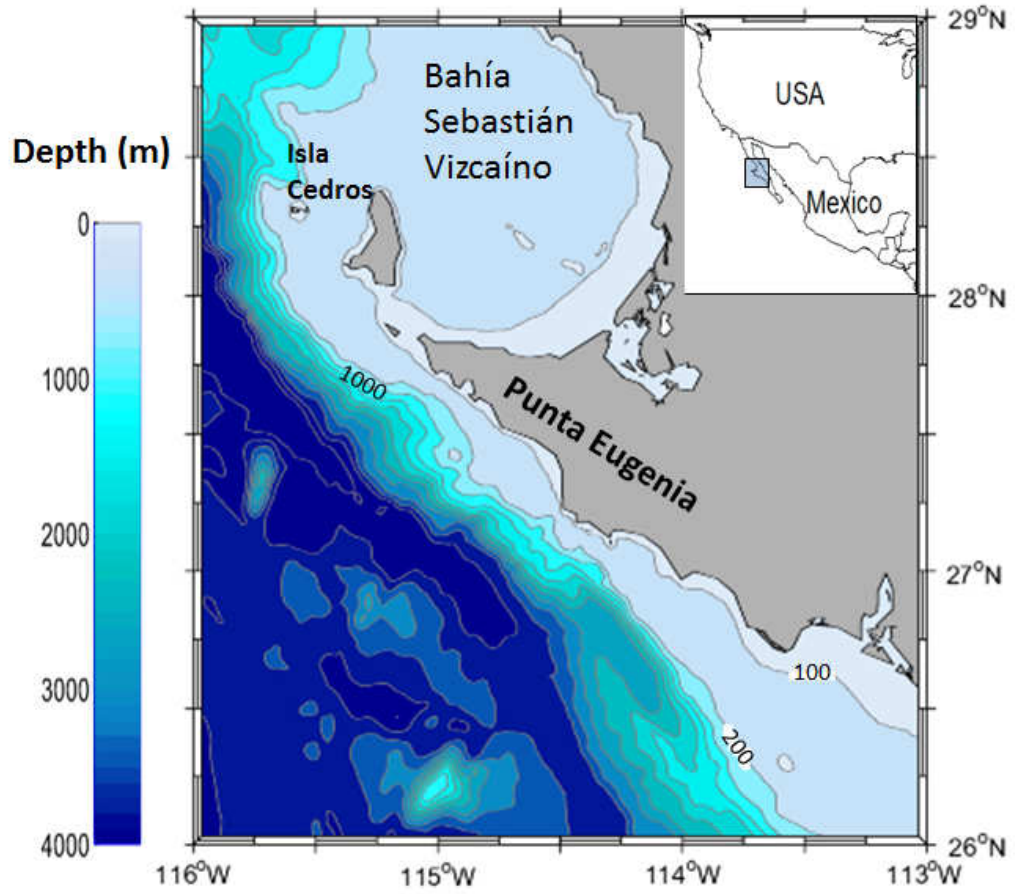


Figure 1. Location and bathymetry characteristics of the study area.

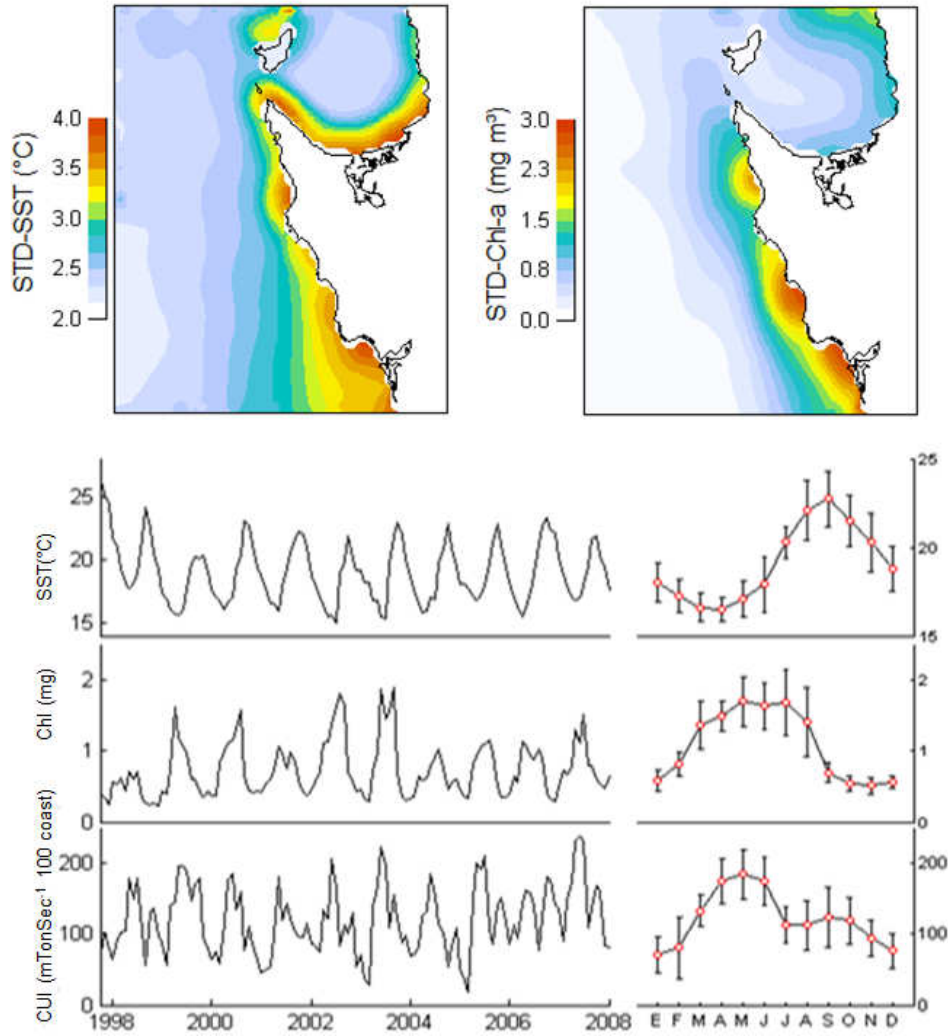


Figure 2. Surface plots of standard deviation variability (time averaged) and monthly time series (spatial averaged) of the satellite-derived SST and Chlorophyll a compared with the monthly CUI time series calculated from the Pacific Fisheries Environmental Group (PFEG) website (<http://www.pfeg.noaa.gov/>) for Punta Eugenia region (27°N, 116°W). The curves on the right side correspond to the average seasonal cycle for each variable. Observed averages (red circles) and vertical bars indicate standard deviation.

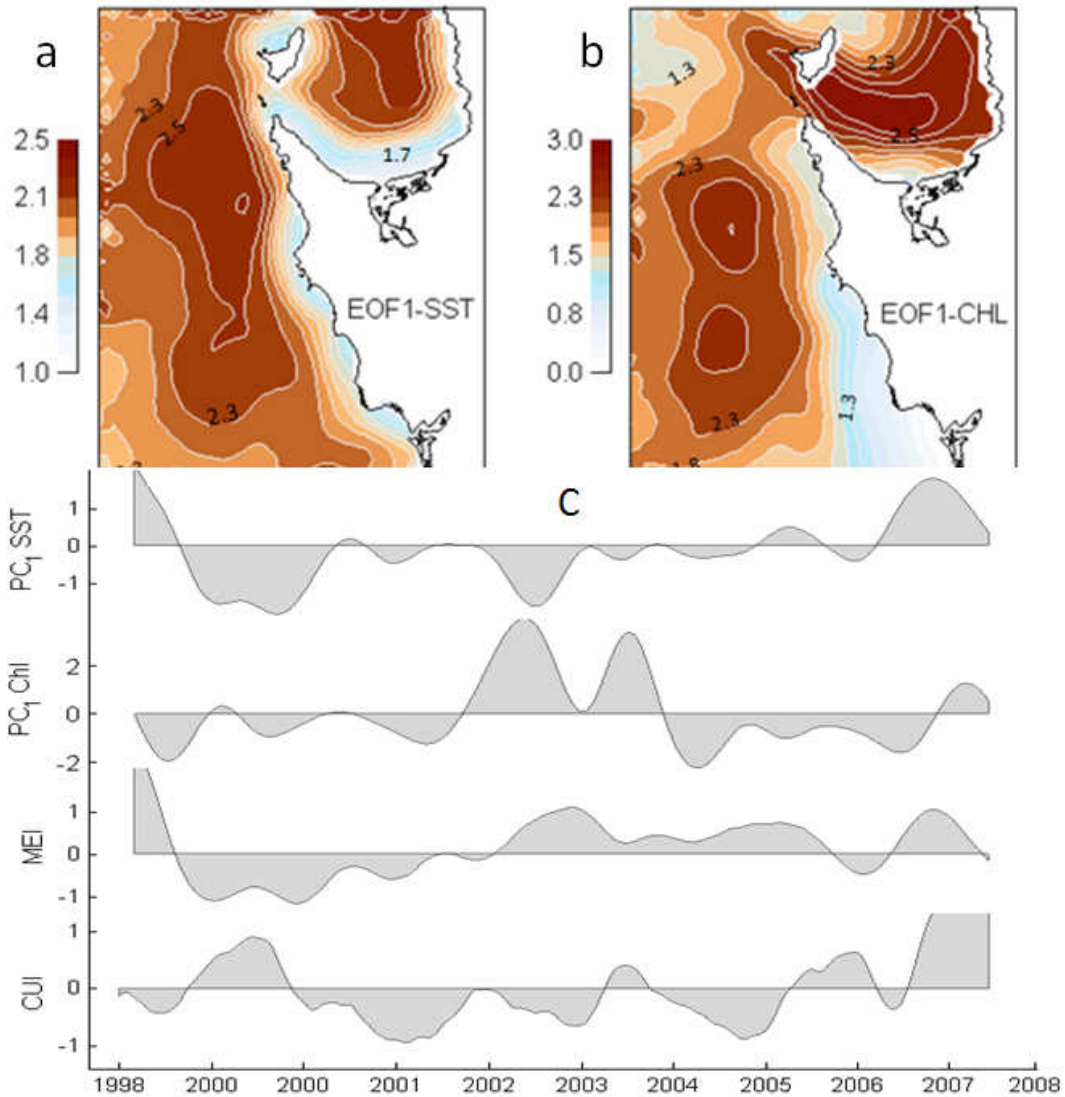


Figure 3. Spatial patterns for mode 1 of the individual EOF analyses. (a) SST, (b) Chlorophyll a. This mode accounts for 78% and 45% of the total variance for SST and Chlorophyll a (with the sign reversed), respectively. (c) Time-series data indicate the temporal evolution of the EOF₁ alongside the MEI and monthly CUI anomalies, all smoothed by a double five-term running mean. $N = 116$ (corresponding to the number of months of smoothed data), the critical value $R_{crit} = (P < 0.05) = 0.319$.

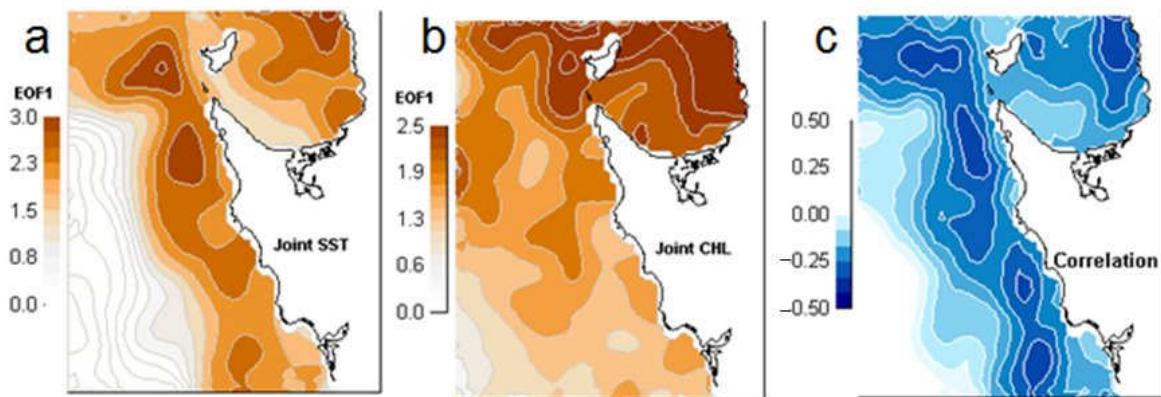


Figure 4. Spatial patterns for mode 1 of the joint EOF analyses of (a) SST, (b) Chlorophyll a (accounting for 80% of the total variance) and (c) correlation map between monthly anomalies of SST and Chlorophyll a. The largest negative correlations (< -0.2 , the blue areas) are seen along the coast and coincide with the high joint EOF₁ scores (>2.0) of SST (a). Absolute correlations above, $R_{crit} (P < 0.05) = 0.211$, (i. e. the strongest negative correlation) are significant at the 95% confidence level.

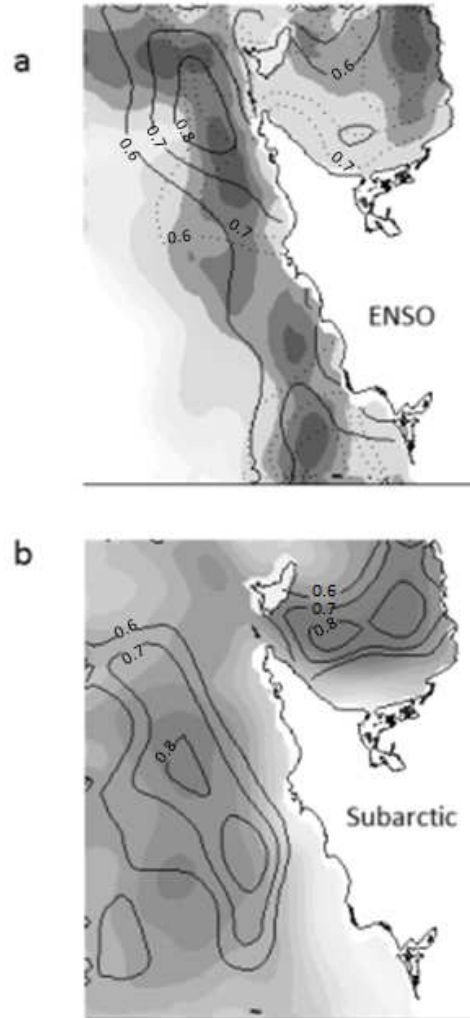


Figure 5. Contours of mean homogeneous correlation overlaid on (a) the correlation map for the El Niño and La Niña period (solid and dotted contours) and (b) for mode 1 Chlorophyll *a* for the intrusion of subarctic water period (solid contours) using data of both SST and Chlorophyll *a*. The El Niño correlation is done using data from September 1997 through December 1998, La Niña correlation is done using data from September 1998 through December 2000 and the subarctic water correlation is done using data from January 2002 through December 2003. The contour interval is 0.1 and the minimum contour shown is 0.6. Absolute correlations above 0.4 are significant at the 95% confidence level.

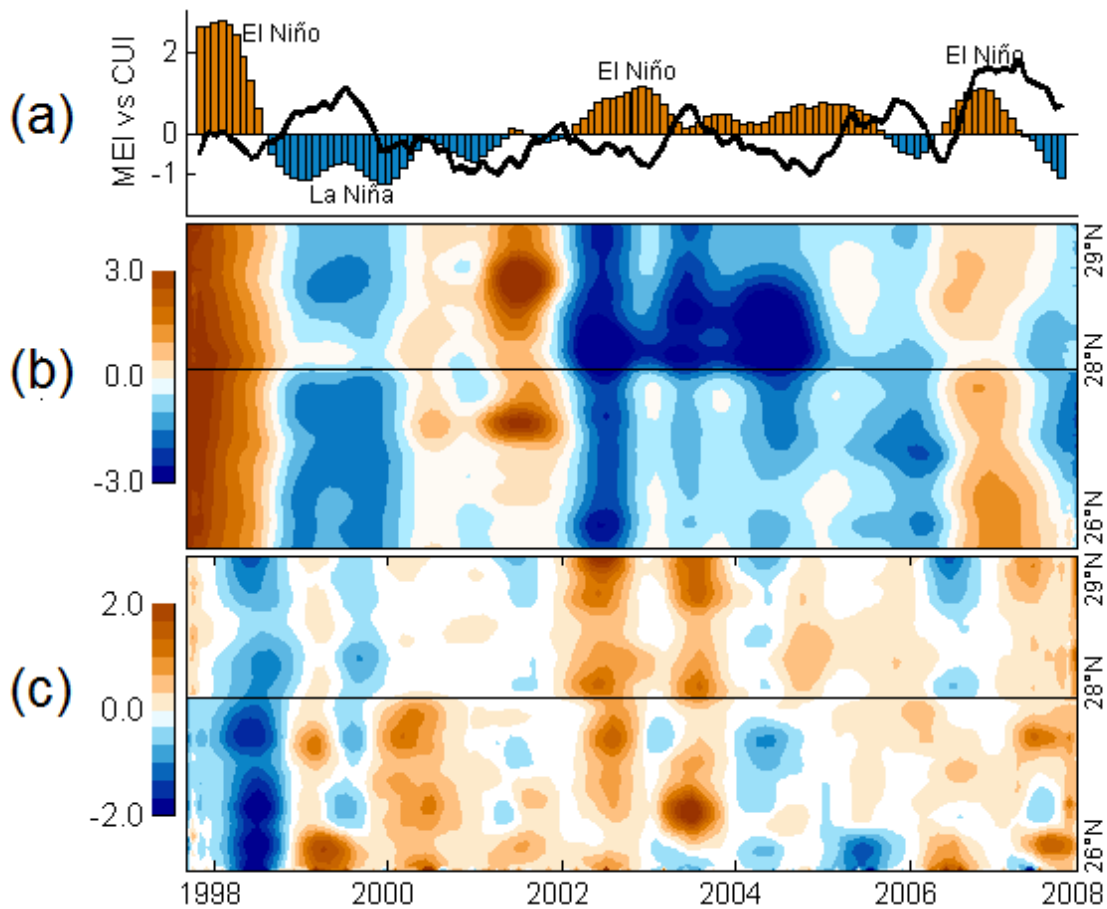


Figure 6. Temporal evolution of (a) the MEI and monthly CUI anomalies. El Niño (La Niña) episodes are indicated by orange (blue) bars respectively as reported by the Climate Prediction Center of the National Center of Environmental Prediction at the National Oceanic and Atmospheric Administration (CPC-NCEP-NOAA). Hovmöller diagram of monthly averaged coastal SST anomalies (b) and Chlorophyll-a anomalies (c), from September 1997 to December 2007, covering approximately 300 km of coastline, from 26°N (bottom graph) to 29°N (upper graph). Solid line, indicates the position of Punta Eugenia in the coast (28°N).

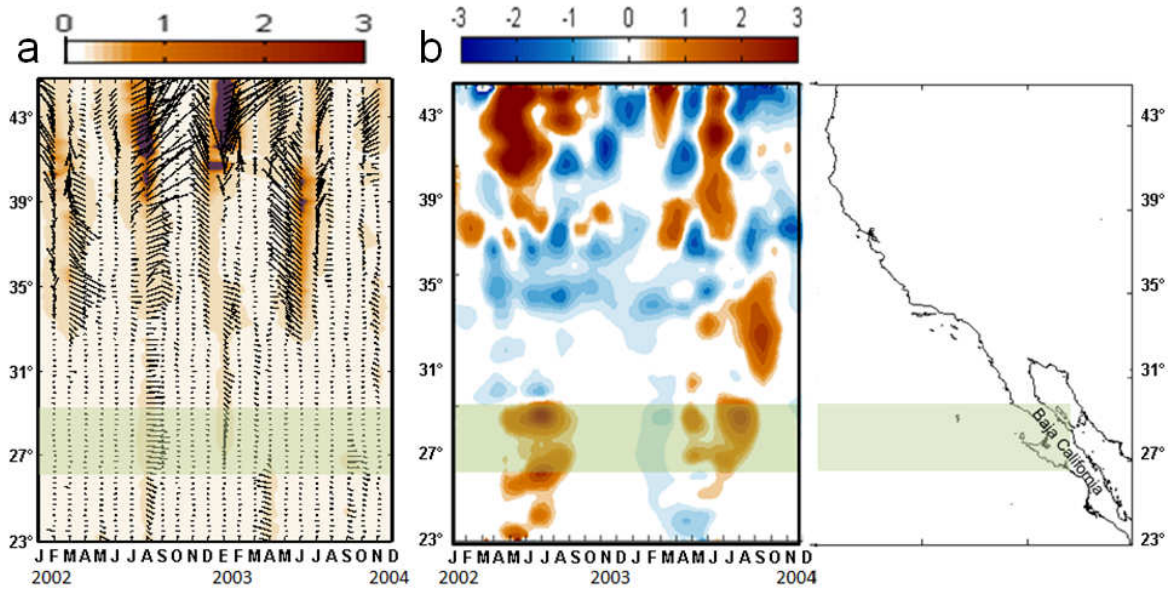


Figure 7. Hovmöller diagrams of interannual anomalies of (a) monthly wind stress (magnitude and direction; $\text{N m}^{-2} \times 10^{-2}$) and (b) weekly Chlorophyll *a* (mg m^{-3}) from January 2002 to December 2003 along the northeast Pacific coast from 22°N to 45°N (values within 50 km of the coast), including Punta Eugenia area (shaded in green). The wind data are provided by the Cross-Calibrated Multi-Platform (CCMP) project website at <http://podaac.jpl.nasa.gov/dataset/>, and weekly Chlorophyll *a* by the SeaWiFS Project of NASA Goddard Space Flight Center website at <http://oceancolor.gsfc.nasa.gov/>.